This is a preprint of an article published in Journal of Testing and Evaluation, Volume 40, Issue 2, Pages 238-242, 2012, DOI: 10.1520/JTE104191, http://www.astm.org

Computer-Controlled Stable Crack Growth as a Reliable and Fast Method to Determine Subcritical Crack Growth

Hüseyin Özcoban [a)], Theo Fett [b)], Gerold A. Schneider [a)+]

a) Institut für Keramische Hochleistungswerkstoffe, Technische Universität Hamburg-Harburg, Hamburg, Germany

b) Institut für Angewandte Materialien - Keramik im Maschinenbau, Karlsruher Institut für Technologie (KIT), Karlsruhe, Germany

[+] Corresponding author: g.schneider@tu-harburg.de

Abstract

Subcritical crack growth of synthetic fused silica glass is investigated using the Single-Edge-V-Notched-Beam (SEVNB) method. The measurement was performed in a very stiff four-point bending device, which is equipped with a computer-aided control system. This technique enables several loading cycles of controlled crack growth with one measurement and sample. The control system is based on an online compliance measurement that enables an automatic measurement routine without much operation of the user and without the necessity of the optical observation of the crack. The crack velocity as a function of the applied stress intensity factor was determined by analysing the measured specimen compliance. The presented method allows determining a large number of v-K_I curves under identical conditions by measuring only one sample.

keywords: subcritical crack growth, stable crack growth, mechanical properties, glass

Introduction

The fracture toughness (K_{Ic}) is a material parameter that characterises the onset of unstable crack propagation. Subcritical crack growth (SCG) causes the crack growth to start even when the applied stress intensity factor is less than the fracture toughness [1,2,3]. SCG is material dependent and depends on the environment and the temperature. This type of crack propagation has to be considered and characterised for an appropriate and reliable application of the used material.

There are several methods for determining the subcritical crack growth behaviour (for an overview see, e.g., Ref [3]). One of them is the bending test. Kleinlein and Wilde et al. [4,5] have earlier performed controlled fracture tests with chevron-notched bending samples to investigate the subcritical crack growth behaviour of macrocracks. The greatest challenge here is to advance the crack in a stable manner. Controlled crack propagation experiments were realized in Refs [4,5] by reducing the load before the point of unstable crack growth in the force-displacement curve was attained. This crucial point was estimated in advance using an estimated K_{Ic} of the material and the corresponding crack length.

In the present study, controlled fracture measurements are described, which were performed in a custom-made bending device that is equipped with a computer-aided control system, which measures the sample compliance online. This enables automatic stable crack growth measurements without much operation of the user. It was already successfully applied to silicon nitride [6,7] to measure extremely steep R-curves and to zirconia-toughened alumina [8] to determine the fracture toughness with automated control of stable crack growth. The advantage of this computer-controlled system is that manifold routine measurements without the necessity of highly qualified research assistants are possible. The automation allows very reproducible and standardised measurements with a high density of data points. Furthermore, compared to the conventional methods, our automated measuring system minimizes the number of needed samples, because stable crack growth is more easily realisable. In principle, the presented method allows determining the v-K_I curve over the whole range. Especially efficient is the method for high crack growth velocities. Such a measurement and the corresponding evaluation of the data can be completed within one day.

As an example, the potential of this method is presented in this article. The Single-Edge-V-Notched-Beam (SEVNB) method is used to determine subcritical crack growth behaviour on synthetic fused silica glass. The experimental procedure, including experimental setup and preparation of the specimen, will be introduced briefly. The theoretical background for calculating the crack velocity at different applied stress intensity factor levels by means of the analysis of the measured compliance will be given. Finally, the result of a sequence of measurements will be presented. The result shows that this method enables determining a large number of v-K_I curves by measuring only one specimen.

Determination of v-K_I curve by means of the measured compliance

Theoretical background

In the following, the theoretical background as well as the used experimental setup is presented briefly to give the basis for evaluating the measured data. The four-point bending test, in particular the SEVNB method, is commonly used to determine the fracture toughness K_{Ic}. If we neglect SCG, the condition for crack growth is fulfilled when the applied stress intensity factor K_I is equal to the fracture toughness K_{Ic}. The applied stress intensity factor K_I for a four-point bending test can be calculated by (see, e.g., Ref [9]):

$$K_I = \frac{3F\,\Delta s\sqrt{\alpha}\;\Gamma(\alpha)}{2bh^{3/2}(1-\alpha)^{3/2}} \tag{1}$$

with $\alpha = a/h$ and $\Delta s = s_2 - s_1$, where s_1 is the inner and s_2 the outer distance of the support rollers, b the width of the specimen, h the height of the specimen, F the applied force, a the actual crack length and, $\Gamma(\alpha)$ the geometric function. If SCG prevails, the criterion for crack growth is not $K_I = K_{Ic}$ anymore, because the crack growth already starts at $K_I < K_{Ic}$. In glass exhibiting the effect of subcritical crack growth, the crack velocity v is strongly affected by the water in the environment [1]. For a material that exhibits slow crack growth, the dependence of the crack velocity on the measured fracture toughness K_I can be characterized by a v-K_I diagram as shown schematically in Fig. 1 [2,3]. In region I, the crack velocity increases with an increasing stress intensity factor and is influenced strongly by the environment. In some cases (e.g., soda-lime glass [10,11]), no SCG was found below the threshold value $K_{I,th}$. In the limit of very high velocities in region III, K_I is equal to the fracture toughness K_{Ic}, which corresponds to the case without subcritical crack growth. For glass, it was also found that, at relatively high crack velocities, v is independent of K_I. This plateau is identified by region II. As the $v(K_I)$ function increases continuously, every crack velocity v corresponds to a specific value of K_I.

The experiments were performed in a very stiff custom-made four-point bending device, which is displacement controlled [12]. The support rollers have distances of 10 mm and 20 mm and a diameter of 5 mm. With this displacement controlled device, crack propagation can be conducted in a stable manner. A key feature of this device is a computer-aided control system that evaluates the slope of the force-displacement curve during the measurement online. Because the compliance of the sample increases as the crack propagates, the information of the actual slope of the force-displacement curve can be used to detect crack propagation even before it can be observed optically on the sample surface [8]. The user sets a critical slope value (representing a well-defined compliance), which is above the initial compliance. As soon as the actual slope of the load-displacement curve reaches this set value, the device unloads automatically. Thus, the crack propagation can be stopped after it has been initiated and before catastrophic failure occurs. After this partial unloading, the measurement is restarted. Herewith, this technique provides the opportunity to perform several loading cycles on one specimen. It should also be mentioned that performing controlled fracture tests on particular brittle materials (like Si_3N_4 [6,7] and zirconia-toughened alumina [8]) were only possible by means of this computer-aided technique and the high stiffness of the device. Especially, materials with constant fracture toughness like glass require an even stiffer device and a faster response time to unload to perform stable crack growth.

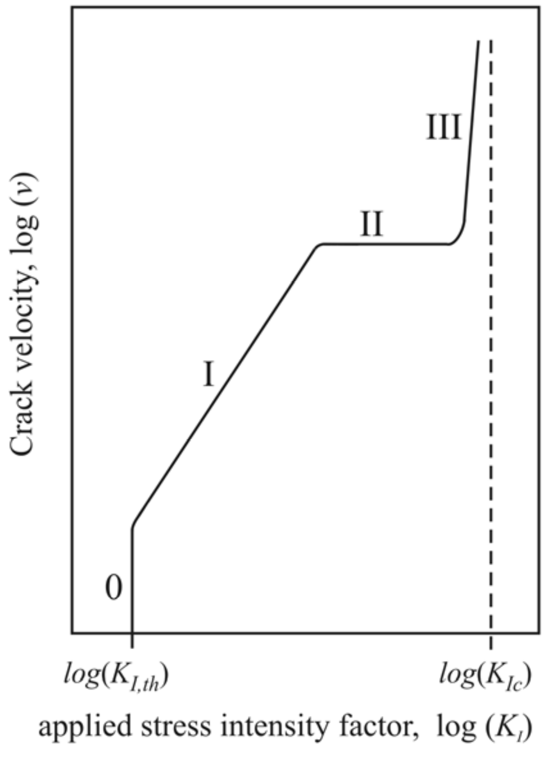

FIG 1: *Schematic v-K_I curve with different crack velocity regions.*

When crack propagation is initiated, the specimen compliance increases with the crack propagation Δl. The change in compliance (ΔC) for a specimen with a notch length of a_0 is given by [13]:

$$\Delta C = \frac{9\Delta s^2}{2Ebh^2}\int_{\alpha_0}^{\alpha}\frac{\alpha'(\Gamma(\alpha'))^2}{(1-\alpha')^3}d\alpha' \qquad (2)$$

where $\alpha_0 = (a_0+l_0)/h$ is the pre-existing total crack length at the beginning of the cycle to be evaluated, $\alpha = \alpha_0 + (\Delta l/h)$ and E is the Young's modulus.

It has to be considered that after sample preparation, crack-like defects already exist ahead of the sharpened notch of notch tip radius r_N, which can be characterised by a pre-crack of length l_0. When crack propagation has been initiated, l_0 extends by subcritical crack growth while the specimen is being loaded. For short pre-cracks ($l_0 < 1.5\ r_N$), Eq 2 is not correct anymore because the obtained results are influenced strongly by the notch effect (see Appendix). The influence disappears when $l > 1.5\ r_N$ (where $l = l_0+\Delta l$) or when r_N is above a critical notch radius r_c, which is material dependent. When the crack propagates for $l < 1.5\ r_N$, the notch effect also has to be considered when determining the change of compliance and the applied stress intensity factor. However, for the presented measurements, it was ensured already after the first partial unloading that $l > 2\ r_N$ and, consequently, the notch influence could be neglected for the following loading cycles. If a large number of cycles can be evaluated it is recommended to extend the crack in the first cycles so that $l > 1.5\ r_N$ is reached. The evaluation of the *v-K* curve can then be simply computed via Eqs (1) and (2). For the case of only a small number of successive loading cycles achievable, the first cycle may also be evaluated by application of the slightly more complicated relations given in the Appendix. In this case, the pre-existing initial crack length has to be obtained from inert strength measurements (see also Appendix).

Evaluation of experimental Data

To keep a clear overview, only the evaluation of the experimental data of the first loading cycle from one measurement with stable crack growth will be shown. The test specimen is a bar with dimensions of about 3 x 5 x 25 mm^3, a notch of length $a_0 = 2.46$ mm, and a notch radius of $r_N = 11.5$ µm prepared by use of a diamond saw blade and sharpened with the razor blade method [14]. The material is a synthetic fused silica glass (SCHOTT - LITHOSIL®, SCHOTT AG, Jena, Germany). The experiment was performed with a constant displacement rate of $v_d = \mathrm{d}C/\mathrm{d}t = 0.01$ µm/s. The displacement Δ_i was measured by using an inductive position encoder, where the force F_i was measured by a quartz sensor (for more details, see Ref [12]).The applied force F_i, as well as the displacement Δ_i at the time t_i, was measured permanently while loading the specimen. Therewith, the actual compliance $C_i = \Delta_i/F_i$ was determined for any recorded data point. In Fig. 2, the force-displacement curve of the first loading cycle is shown.

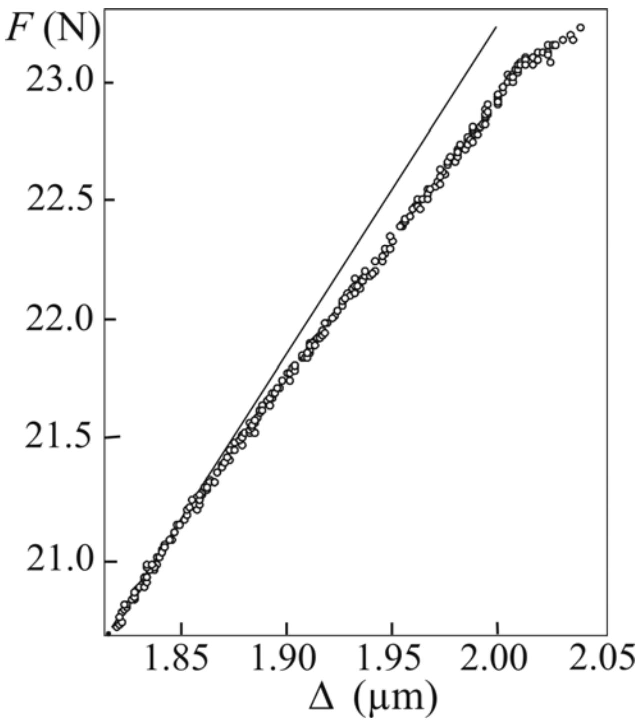

FIG 2: *The relevant force-displacement curve range of the first loading cycle. The solid line was fitted by the data points in the force range of 17 N < F < 21 N.*

At an applied force of almost 23.3 N, the device has unloaded automatically because the specimen compliance had changed more than the set value. After the partial unloading, the control system of the device is restarted manually. Pilot tests have shown that even when the set compliance value was increased by up to a factor of 2, the attained maximal force does not change within the experimental scatter of the data points. This can be explained by the fact that the crack velocity at those applied stress intensity factor is relatively high, and therefore the specimen compliance changes very quickly. The device has to unload very fast to avoid catastrophic failure. The solid line was obtained by linear regression of the data in the force range of 17 N < F < 21 N. To show the first visible change in specimen compliance, only the relevant range of the force-displacement curve is given in Fig. 2. The measured data starts to deviate remarkably from the straight-line fit at ~ 21.3 N, which indicates that crack propagation has been initiated. The change in compliance $\Delta C_i = C_i - C_0$ was calculated for any data set (F_i, Δ_i, t_i), where C_0 corresponds to the inverse of the slope of the straight-line fit in Fig. 2. Knowing the increase of compliance, the crack propagation Δl_i was calculated by solving numerically Eq 2 with respect to the upper integration limit [6]. Thus, the crack propagation was calculated for every t_i. The crack propagation of the second loading cycle (the first evaluated one of a series of cycles) is shown in Fig. 3.

The crack velocity was determined by means of the fit function $l^{+}(t)$ for two neighbouring data points (i) and (i-1) by $v_i = (l^{+}(t_i)\text{-}\ l^{+}(t_{i-1}))/(t_i\text{-}t_{i\text{-}1})$.

The applied stress intensity factor $K_{I,i}$ was computed through the applied force F_i and the corresponding crack length $a_i = a_0 + l_0 + \Delta l_i$ by using Eq 1 (see Appendix). By knowing the final crack propagation from the nth loading cycle l_{n}, the lower integration limit (Eq 2) for the following loading cycle was taken as $l_{0,\mathrm{n}+1} = l_{\mathrm{n}}$, and the next loading cycles were calculated accordingly.

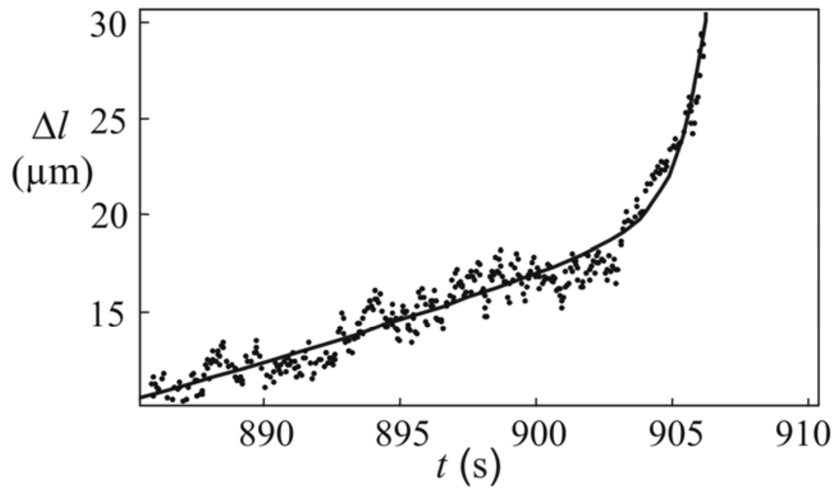

FIG 3: *The crack propagation Δl for the first evaluated loading cycle (the second cycle recorded). Here the time starting point is arbitrarily chosen. Every point is calculated by solving numerically Eq 2, and the results are fitted with the fit-relation* $l^{+}(t) = 4.1\times10^{-11}\exp(-0.999t) + 0.00406(t+42)^{2}$ (l^{+} *in μm for t in s*).

In Fig. 4, the v-K_I curves are shown. For the sake of clarity, only the first six loading cycles are presented by open circles.

Wiederhorn and Bolz [10] have observed that the crack growth behaviour of glass in water is mainly dominated by the region I of crack growth. Furthermore, Wiederhorn [11] has demonstrated by measurements on soda-lime glass that the subcritical crack growth behaviour of glass in air is different than in water. In Fig. 4, the v-K_I curves of fused silica published by Suratwala and Steele [15] are plotted as solid lines. They have investigated the influence of air humidity on the subcritical crack growth behaviour in fused silica using the double cantilever-drilled compression method. It was shown that the crack velocity increases with the water vapour concentration in the atmosphere. Additionally, fused silica showed regions I, II and III of crack growth. The solid lines in Fig. 4 represent various P_{H2O} ranging from 0.3 to 120 Pa at 25°C.

The results of the present study (represented by open circles in Fig. 4) also show a region where the crack growth velocity is almost constant. Above an applied stress intensity factor of nearly

K_I = 0.62 MPa√m, the crack velocity is a strongly increasing function of K_I. It is remarkable that all loading cycles in this region exhibit an almost identical slope. In principle, any desired number of loading cycles can be performed as long as the crack propagates in a stable manner.

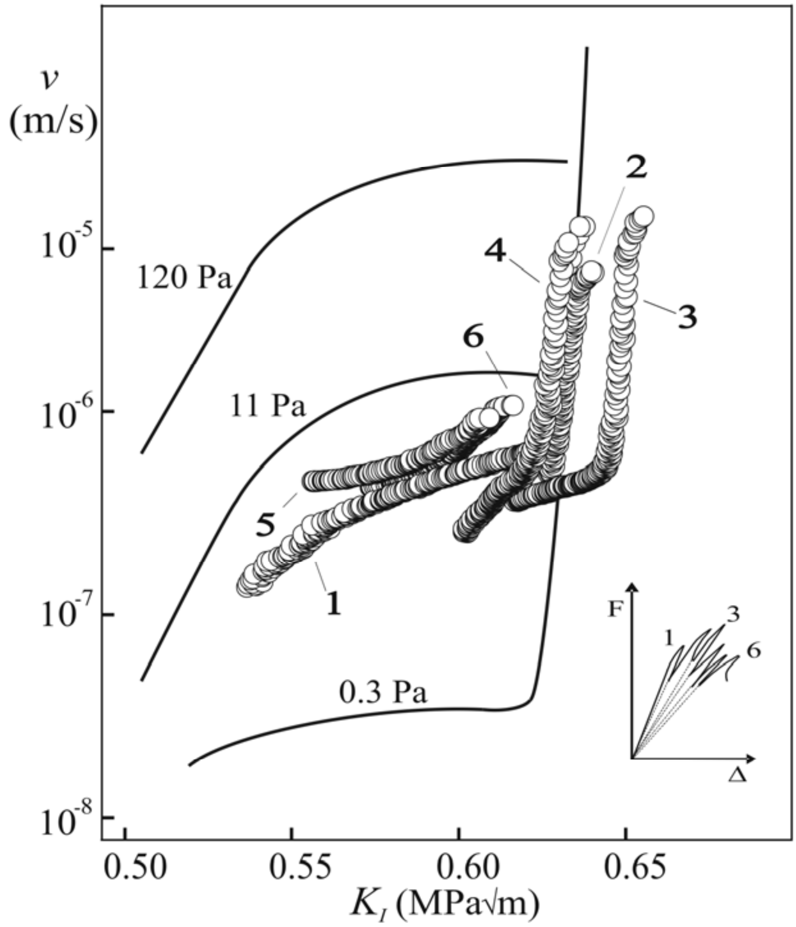

FIG 4: *The open circles represent the v-K_I curves of the first six loading cycles. The corresponding force-displacement curve is shown schematically and the loading cycles are numbered accordingly. The experiments were performed in normal labour conditions. The solid lines are v-K_I curves at 25°C at various P_{H2O} ranging from 0.3 to 120 Pa published by Suratwala and Steele* [*15*]. *(From the differences of the presented curves representative for a larger number of curves, the reproducibility can be estimated as ΔK<0.02 MPa √m and Δlg_{10}(v)<0.1.)*

Summary

The subcritical crack growth behaviour of synthetic fused silica glass was investigated by using the SEVNB method. Because of the high stiffness of the loading device and the computer-aided control system, several loading cycles with stable crack growth were performed with one sample. Measuring online the specimen compliance, v-K_I curves in the range of $10^{-7} < v < 10^{-5}$ m/s were determined. Hereby, the v-K_I curve exhibits a region of almost constant crack velocity v, where v increases strongly at an applied stress intensity factor close to $K_I = 0.62$ MP√m. In our opinion, the combination of a very stiff loading device combined with an online compliance measurement, which enables stable crack growth by a computer-aided control, is a major steep forward to a user-friendly very reliable subcritical crack growth measurement.

Acknowledgments

The writers thank Dipl.-Ing. V. Salikov from the Hamburg University of Technology for sample preparation and preliminary experiments.

Appendix

A major limitation that has to be considered in determining the fracture toughness K_{Ic} with the SEVNB method is the occurrence of a finite notch radius r_N. The stress intensity factor formally computed by Eq 1, in the following abbreviated by $K^{(1)}$, postulates the existence of a crack of total length $a = a_0+l$, i.e., this relation interprets the notch part as part of a crack.

In presence of a notch with length a_0, the stress intensity factor for the crack emanating from the notch root having the length l is given by

$$K_I(l) = K_I^{(1)}(a_0 + l)\tanh\left(2.243\sqrt{\frac{l}{r_N}}\right) \tag{A1}$$

From this relation, it becomes clear that for l larger than ≈1.5-2 r_N, the true and the formally computed stress intensity factors agree [16].

For cracks with $l < 1.5\ r_N$, Eq 1 must lead to an overestimation when determining the fracture toughness by the assumption of a crack of total length a_0+l. The magnitude of the notch effect depends on the notch radius r_N and the crack length l in front of the notch.

This means that for short precracks ($l < r_N$), the applied force for crack growth must be much higher than that calculated by Eq 1 to compensate for the notch effect, which leads to a kind of "stress shielding" of the pre-crack.

Damani et al. have shown that crack-like defects already exist ahead of the sharpened notch before the sample is mechanical loaded [17,18]. They discuss them as defects that are introduced while the sample is being notched and can be described by their initial pre-crack length l_0, as shown schematically in Fig. 5.

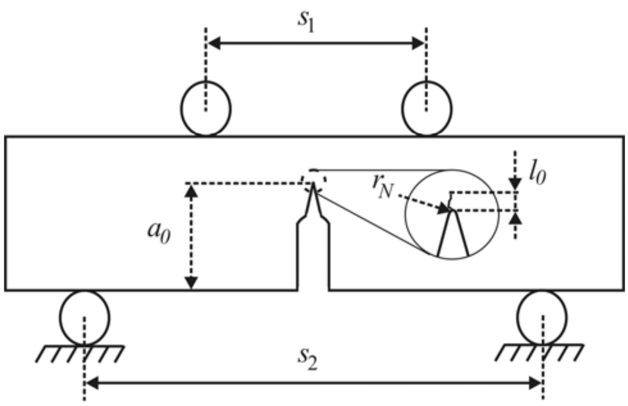

***FIG 5**: Schematic four-point bending setup without external mechanical load. The sample has a pre-crack length l_0 in front of a notch with the length a_0.*

While the sample is loaded, the pre-crack length l_0 extends by subcritical crack growth. The amount of overestimation caused by the notch effect is determined by l and the notch radius r_N. The influence becomes insignificant when the pre-crack has propagated more than $l^* = l_0 + \Delta l = 1.5\ r_N$ [16]. Because l_0 is not known exactly, the influence of the finite notch root radius cannot be estimated accurately. Therefore, it is recommended that the prepared notch radius is as small as possible. Pilot tests on synthetic fused silica glass with different notch radii have shown that below a critical value of $r_c \approx 12$ µm the results were not influenced anymore by the notch radius. Because the prepared notch radius of the investigated specimen is below r_c, the influence of the notch radius can be neglected in the presented measurement. Furthermore, the fracture toughness K_{Ic} of the investigated silica glass was determined by performing fast measurements (displacement ratio of $v = 5$ µm/s) with notch radii below 12 µm. The obtained fracture toughness is equal to $K_{Ic} = 0.82$ MPa√m, which matches very well with the value given in the literature [19]. Based on Eq A1 and the pilot test with different notch radii, a reasonable pre-crack length of $l_0 = 15$ µm can be assumed for a specimen with a notch radius of $r_N \approx 12$ µm.

The increase in compliance including the influence of notch effect (ΔC_N) is given by [13]:

$$\Delta C_N = \frac{9\,\Delta s^2}{2\,E\,b\,h^2} \int_{\alpha_0}^{\alpha} \frac{\alpha' \left(\Gamma(\alpha')\right)^2}{(1-\alpha')^3}\ tanh^2\left(2.243\ \sqrt{\frac{l}{r_N}}\right) d\alpha' \qquad \text{(A2)}$$

where $l > l_0$.

It has to be mentioned that for materials which exhibit an increasing fracture toughness, the R-curve has also to be considered in order to calculate the correct crack length [3].

References

[1] Wiederhorn, S., Subcritical crack growth in glass. In: Bradt, R. C., Hasselman, D. P. H. & Lange, F. F., Editors, Fracture Mechanics of Ceramics vol. 4, Plenum Press, New York, 1978, 549-580.

[2] Lawn, B. R., Fracture of Brittle Solids – Second Edition. Cambridge Solid State Science Series. Cambridge University Press, 1993.

[3] Munz, D., Fett, T., Ceramics. Mechanical Properties, Failure Behavior, Material Selection. Springer-Verlag, Berlin Heidelberg New York, 1999.

[4] Kleinlein, F.W., Langsame Rissausbreitung in spröden Werkstoffen im Biegeversuch, doctoral thesis, University of Erlangen, Germany (1980).

[5] Wilde, J, Groll, W. and Kleinlein, F.W., "Measurement of crack propagation data in small slices of brittle materials in controlled bending" J. Mater. Sci., Vol. 20, 1985, pp. 4096-4074.

[6] Fett, T., Fünfschilling, S., Hoffmann, M.J., Oberacker, R., Jelitto, H. and Schneider, G.A., "R-curve Determination for the Initial Stage of Crack Extension in Si_3N_4" J. Am. Ceram. Soc., Vol. 91, 2008, pp. 3638-3642.

[7] Fünfschilling, S., Fett, T., Oberacker, R., Hoffmann, M.J., Özcoban, H., Jelitto, H., Schneider, G.A. and Kruzic, J.J., "R-Curves from Compliance and Optical Crack-Length Measurements," J. Am. Ceram. Soc., Vol. 93, 2010, pp. 2814-2821.

[8] Özcoban, H., Jelitto, H. and Schneider, G. A., "Influence of finite notch root radius and optically determined crack length on the measured fracture toughness of brittle materials," J. Eur. Ceram. Soc., Vol. 30, 2010, pp. 1579-1583.

[9] Fett, T. and Munz, D., Stress Intensity Factors and Weight Functions, Computational Mechanics Publications, Southampton, 1997.

[10] Wiederhorn, S. M. and Bolz, L. H., "Stress corrosion and static fatigue of glass," J. Am Ceram. Soc., Vol. 53, 1970, pp. 543-548.

[11] Wiederhorn, S. M., "Influence of Water Vapor on Crack Propagation in Soda-Lime Glass," J. Am. Ceram. Soc., Vol. 50, 1967, pp. 407-414.

[12] Jelitto, H., Felten, F., Swain, M. V., Balke, H. and Schneider, G.A., "Measurement of the Total Energy Release Rate for Cracks in PZT Under Combined Mechanical and Electrical Loading," J. Appl. Mech., Vol. 74, 2007, pp. 1197-1211.

[13] Fett, T., "Notch effect in determination of fracture toughness and compliance," Int. J. Fract., Vol. 72, 1995, R27-R30.

[14] Kübler, J., Fracture Toughness of Ceramics Using the SEVNB Method: From a Preliminary Study to a Standard Test Method. Fracture Resistance Testing of Monolithic and Composite Brittle Materials, ASTM STP 1409, J. A. Salem, M. G. Jenkins, and G. D. Quinn, eds., American Society for Testing and Materials, West Conshohocken, PA, 2002, 93-106.

[15] Suratwala, T. I. and Steele, R. A., "Anomalous temperature dependence of sub-critical crack growth in silica glass. J. Non-Cryst. Solids," Vol. 316, 2003, pp. 174-182.

[16] Fett, T., "Influence of a notch root radius on fracture toughness," J. Eur. Ceram. Soc., Vol. 25, 2005, pp. 543-547.

[17] Damani, R. J., Gstrein, R. and Danzer, R., "Critical notch-root radius effect in SENB-S fracture toughness testing," J. Eur. Ceram. Soc., Vol. 16, 1996, pp. 695–702.

[18] Damani, R.J., Schuster, Ch. and Danzer, R., "Polished Notch Modification of SENB-S Fracture Toughness Testing," J. Eur. Ceram. Soc., Vol. 17, 1997, pp. 1685-1689.

[19] Wiederhorn, S. M., "Fracture Surface Energy of Glass," J. Am. Ceram. Soc., Vol. 52, 1962, pp. 99-105.